ChemCatChem
Research Article
doi.org/10.1002/cctc.202200129
Chemistry Europe
European Chemical Societies Publishing
www.chemcatchem.org

Aluminum-Containing Metal-Organic Frameworks as Selective and Reusable Catalysts for Glucose Isomerization to Fructose

Mohammad Shahinur Rahaman,[a] Sarttrawut Tulaphol,[b] Anwar Hossain,[a] Jacek B. Jasinski,[c] Shashi B. Lalvani,[d] Mark Crocker,[e] Thana Maihom,[f] and Noppadon Sathitsuksanoh*[a]

Fructose is a versatile precursor for food and chemicals. Currently, catalytic production of fructose is achieved by enzymatic isomerization of glucose from renewable lignocellulose. Although the catalyst, glucose isomerase, is selective, it is not stable. Here, aluminum-containing metal-organic frameworks (Al-MOFs) are shown to be active, selective, stable, and reusable for glucose isomerization in ethanol. Al-MOFs achieved 64% fructose selectivity with 82% glucose conversion at 120 °C, superior performance compared with most other solid catalysts. The amino groups in Al-MOFs enhance Lewis acid strength, which is responsible for the high fructose selectivity at high glucose conversion. Moreover, the Al-MOF catalyst is stable and reusable at least four times without losing either activity or fructose selectivity. These findings illustrate compelling opportunities for Al-MOFs in fructose production and other organic reactions, such as fructose conversion to 5-hydroxymethylfurfural and levulinic acid.

Introduction

Fructose is an essential precursor for food/beverages,[1] such as fructose syrup and soft drinks, and for chemical feedstocks, such as 5-hydroxymethylfurfural, levulinic acid, and lactic acid.[2–3] Currently, sugar mills produce fructose by enzymatic isomerization of glucose catalyzed by immobilized glucose isomerase. The glucose isomerase yields 42% fructose (>84% fructose selectivity), 50% glucose, and 8% other saccharides.[4] Although selective, enzyme-based production has several drawbacks, particularly a requirement for narrow operating conditions (pH and temperature),[5–6] a high cost of the enzymes,[7] and enzyme inactivation.[8] Homogeneous catalysts, such as chromium and aluminum chloride salts, are effective glucose isomerization agents. However, homogeneous catalysts require an extra step of separating the catalyst from the product. Sn-containing β,[8–10] MFI,[11] and MCM-41 zeolites,[12] are effective for glucose isomerization and showed >50% fructose selectivity. However, zeolite synthesis is complex and requires long crystallization times.[8] Moreover, the instability of these zeolites is a major challenge.[13] Thus, the industry needs efficient and stable heterogeneous catalysts for glucose isomerization.

Metal-organic frameworks (MOFs) have drawn attention as heterogeneous catalysts for biomass transformation reactions.[14] MOFs are constructed by coordination linkages between secondary building unit (SBU)/metal clusters and organic linkers.[15–16] The presence of coordinatively unsaturated metal sites within MOFs provides Lewis acid sites that catalyze various reactions, such as acetalization,[17–18] hydrogenation,[19–20] esterification,[21–22] and isomerization.[23–25] Researchers have used various MOF catalysts for glucose isomerization (Table S1). For example, Mello et al.[26] used UiO-66(Zr) in 1-propanol and obtained 72% fructose selectivity at 82% glucose conversion at 90 °C. Oozeerally et al.[27] applied UiO-66(Zr) that yielded <60% fructose selectivity at 16% glucose conversion in water at 140 °C. Akiyama et al.[28] showed that MIL-101(Cr)–SO_3H was active in the water with 27% selectivity to fructose at 78% glucose conversion. Yabushita et al.[29] used NU-1000(Zr) for glucose isomerization in water at 140 °C for 5 h and observed 19% fructose yield at 60% glucose conversion (32% fructose selectivity). Oozeerally et al.[30] used ZIF-8 for the glucose isomerization in water and observed 65% fructose selectivity at 24% glucose conversion at 100 °C.

The glucose isomerization reaction proceeds over Lewis acid catalysts.[31–33] Aluminum-containing MOFs (MIL-53 and

[a] M. S. Rahaman, A. Hossain, Prof. N. Sathitsuksanoh
Department of Chemical Engineering
University of Louisville
Louisville, KY 40292 (USA)
E-mail: n.sathitsuksanoh@louisville.edu
Homepage: http://tikgroup.org
[b] Dr. S. Tulaphol
Department of Chemistry
King Mongkut's University of Technology Thonburi
Bangkok 10140 (Thailand)
[c] Dr. J. B. Jasinski
Conn Center for Renewable Energy Research,
University of Louisville
Louisville, KY 40292 (USA)
[d] Prof. S. B. Lalvani
Department of Chemical, Paper, and Biomedical Engineering,
Miami University
Oxford, OH 45056 (USA)
[e] Prof. M. Crocker
Department of Chemistry
University of Kentucky
Lexington, KY 40506 (USA)
[f] Dr. T. Maihom
Department of Chemistry
Kasetsart University
Nakhon Pathom 73140 (Thailand)

Supporting information for this article is available on the WWW under https://doi.org/10.1002/cctc.202200129

MIL-101) have Lewis acidic Al centers for catalyzing glucose isomerization to fructose. Thus, we expected that aluminum-containing MOFs would generate active Lewis acidic Al sites for glucose isomerization. However, the catalytic performance of Al-containing MOF (Al-MOF) catalysts for glucose-fructose isomerization in alcohols was unknown.

The objective of this work was to evaluate aluminum-containing MOF (Al-MOF) catalysts for glucose isomerization in ethanol (Scheme 1). Among Al-MOFs, MIL-101(Al)-NH_2 gave a high fructose selectivity of 64% at 82% glucose conversion. The presence of amino groups enhanced medium-to-strong Lewis acid strength, fructose selectivity, and glucose conversion. Moreover, MIL-101(Al)-NH_2 MOF was stable and reusable up to four times without losing catalytic performance. The knowledge gained from this work will guide the design of MOF catalytic systems for active and selective glucose-fructose isomerization by biorefineries.

Results

We synthesized three aluminum-containing metal-organic frameworks (Al-MOFs), MIL-101(Al)-NH_2, MIL-53(Al)-NH_2, and MIL-53(Al). Then we evaluated their catalytic performance for glucose isomerization in ethanol. We chose ethanol as a solvent because ethanol shifted the isomerization equilibrium to the fructose side,[34–36] which enabled us to evaluate and compare isomerization ability of different Al-MOF catalysts.

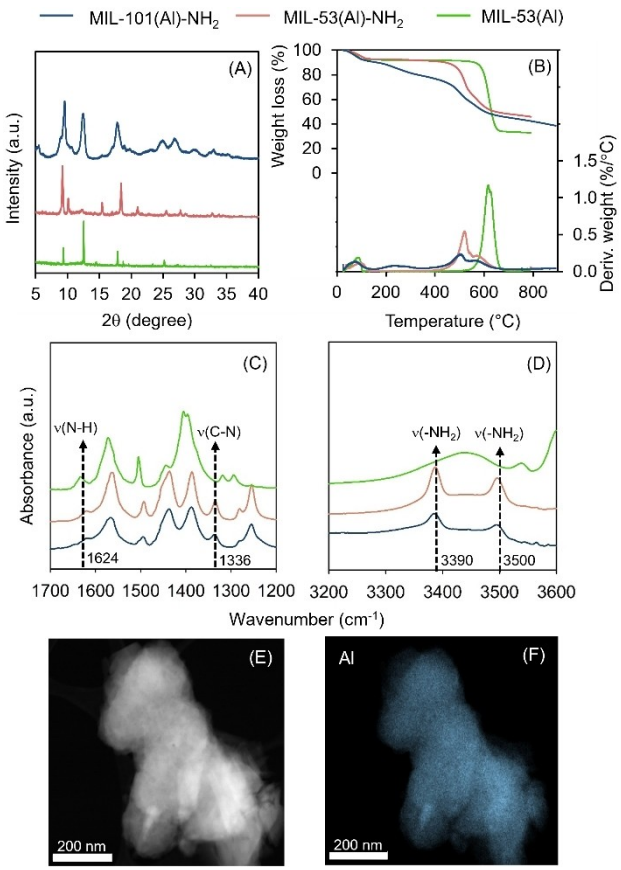

Figure 1. Physicochemical properties of MIL-101(Al)-NH_2, MIL-53(Al) and MIL-53(Al)-NH_2 by XRD (A), TGA (B), FTIR (C and D), HRTEM image of MIL-101(Al)-NH_2 (E), and aluminum mapping of MIL-101(Al)-NH_2 (F)

Characterization of physiochemical and acidic properties of Al-MOFs

To characterize the physiochemical properties, we analyzed the synthesized Al-MOFs by XRD, TGA, FTIR, HRTEM, and N_2 adsorption-desorption measurements (Figure 1 and Figure S1). The metal content was determined by ICP-OES (Table S2).

Figure 1A shows the XRD patterns of MIL-101(Al)-NH_2, MIL-53(Al), and MIL-53(Al)-NH_2. The XRD patterns for the prepared Al-MOFs were similar to reported patterns.[37–42] The N_2 adsorption isotherm of the synthesized MIL-101(Al)-NH_2 showed a type IV isotherm (Figure S1),[43] which suggested that the MIL-101(Al)-NH_2 was a mesoporous material. The calculated surface area and pore volume were 1487 m^2/g and 0.92 cc/g, respectively, similar to reported values.[43–48] To determine the thermal stability of the Al-MOFs, we performed TGA (Figure 1B). The TGA profile of MIL-101(Al)-NH_2 exhibited three mass loss zones, namely at 30–150 °C (~10 wt.%), 150–400 °C (14 wt.%) and 380–800 °C (35 wt.%). These zones corresponded to mass loss resulting from: (1) the evaporation of water molecules, (2) the degradation of organic linkers, and (3) the degradation of the organic 2-aminoterephthalic acid-Al^{3+} complexes. The TGA profile of MIL-53(Al) exhibited two mass loss zones, namely at 30–150 °C (~7.8 wt.%), and 550–700 °C (57 wt.%). The TGA profile of MIL-53(Al)-NH_2 exhibited two mass loss zones, namely at 30–150 °C (~7.2 wt.%), and 430–650 °C (41 wt.%). These two zones corresponded to mass loss resulting from: (1) the evaporation of water molecules, and (2) the degradation of organic linker-Al^{3+} complexes which matched the literature.[41]

Scheme 1. Glucose isomerization to fructose by MIL-101(Al)-NH_2.

To characterize their surface functional groups, we analyzed Al-MOFs by ATR-FTIR (Figure 1C–D). The shoulder at 1336 cm^{-1} can be assigned to the C–N stretching absorption of aromatic amines. These bands confirmed the presence of –NH_2 groups in MIL-101(Al)-NH_2 and MIL-53(Al)-NH_2.[46] The ATR-FTIR spectrum showed bands that corresponded to the symmetric and asymmetric stretching of primary amines (3390 and 3500 cm^{-1}) (Figure 1D), which indicated the presence of –NH_2 functional groups that were uncoordinated. As a control, MIL-53(Al) was evaluated by FTIR and did not show any –NH_2 and C–N bands. HRTEM measurements with elemental mapping demonstrated that MIL-101(Al)-NH_2 was porous with well-dispersed aluminum species (Figure 1E–F). The Al content measured by ICP-OES was

11.6 wt.% (Table S2). Overall, these characteristics matched reported values[43–48] and confirmed the formation of the MIL-101(Al)-NH_2 structure.[43,48]

To probe the acid properties, we performed DRIFTS with adsorbed pyridine on three Al-MOF catalysts. We chose pyridine as an in-situ titrant for probing the Lewis acid site density of MOFs because of previous success in measuring Lewis acid sites in MOFs.[17,49–50] To avoid degradation of these three MOFs, we performed DRIFT in the range of 30–150 °C according to their thermal stability in TGA analysis. After pyridine adsorption, the DRIFT spectra of these MOFs had characteristic bands at 1067 and 1050 cm^{-1} (Figure 2), which corresponded to the coordination between pyridine and coordinated unsaturated sites (CUSs).[50–51] This coordination provided the vital Lewis acid sites (LAS) that interacted with pyridine. Determination of acid properties of MOFs can be difficult. Common acid titration techniques, such as NH_3-TPD,[52] TGA-TPD,[53–54] and dynamic IR[55–56] using various titrants (pyridine,[49,57] acetonitrile,[50] 2,6-di-tert-butylpyridine[58]) typically require high desorption temperatures (> 400 °C). However, MOFs decompose at such high temperature.

The numbers of MOF Lewis acid sites were calculated from the integrated area of the bands (after background subtraction) of adsorbed pyridine at 1067 cm^{-1}. An increase in the desorption temperature from 30–150 °C enabled identification of weak and medium-to-strong Lewis acid sites of MOFs. The intensity of this band decreased with increasing desorption temperature for all the MOFs. The 1067 cm^{-1} band almost disappeared completely at 150 °C for MIL-53(Al), which indicated that this MOFs had weak Lewis acid sites. Conversely, the amino-functionalized MOFs displayed a stronger 1067 cm^{-1} band at 150 °C, which suggested that they had stronger Lewis acid sites compared with their amino-free isostructural counterparts.[57,59] We calculated the Lewis acid site density of MOFs using the peak area of 1067 cm^{-1}. The calculated total Lewis acid site density was in the order MIL-101(Al)-NH_2 (90 a.u./g) > MIL-53(Al)-NH_2 (52 a.u./g) > MIL-53(Al) (44 a.u./g). Interestingly, the $-NH_2$ groups of MIL-53(Al)-NH_2 and MIL-101(Al)-NH_2 gave a high density of medium-to-strong Lewis acid sites, compared with that of MIL-53(Al).

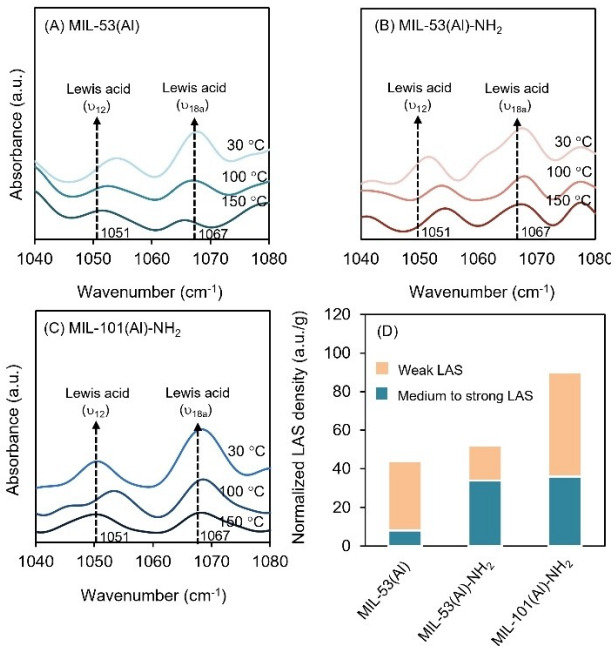

Figure 2. DRIFTS spectra with temperature programmed desorption of pyridine from MIL-53(Al) (A), MIL-53(Al)-NH_2 (B), MIL-101(Al)-NH_2 (C) and normalized Lewis acid site density (D).

Catalytic performance of amino-functionalized metal-organic frameworks

Because we expected that a high density of medium-to-strong Lewis acid sites improved the fructose selectivity, we conducted glucose isomerization using the synthesized Al-MOFs in ethanol at 120 °C (Table 1). The catalyst loading was based on their aluminum content to understand the meaning of metal sites in catalytic performance. As a control, a blank experiment (no added catalyst) showed 8.1 wt.% glucose conversion. However, we did not observe fructose in the control reaction after 2 h, which suggested that glucose isomerization required a catalyst. The synthesized Al-MOFs were active for glucose conversion. Among all the MOFs tested, MIL-101(Al)-NH_2 demonstrated the highest specific activity and productivity of 36 h^{-1} and 20 h^{-1}, respectively. Interestingly, we observed that amino groups (-NH_2) in MIL-53(Al)-NH_2 increased both specific activity and productivity compared with the amino-free isostructural MOF(MIL-53(Al)). The orders of specific activity and productivity were the same as the order of Lewis acid strengths (Figure 2).

To evaluate the catalytic activity, we performed glucose isomerization for 4 h with the three Al-MOFs (Figure 3A–C). We observed glucose conversion and fructose selectivity with a trend similar to the trends for specific activity and productivity. MIL-101(Al)-NH_2 yielded 64% fructose selectivity at 82% glucose conversion after 4 h. To compare the quality of aluminum sites of these Al-MOF catalysts, we plotted the fructose selectivity vs. glucose conversion (Figure 3D). MIL-101(Al)-NH_2 and MIL-53(Al)-NH_2 had the highest selectivity of fructose (50–64%) at ~25–82% glucose conversion. Whereas the MIL-53(Al) had lower selectivity to fructose compared with MIL-101(Al)-NH_2 and MIL-53(Al)-NH_2 at all conversions. These results suggested that (1) MIL-101(Al)-NH_2 and MIL-53(Al)-NH_2 had similar quality of aluminum active sites, and (2) amino groups improved glucose conversion and fructose selectivity. Overall, these results

Table 1. Catalyst screening for glucose isomerization.

Catalyst	Specific activity[a] [h^{-1}]	Productivity[a] [h^{-1}]
MIL-101(Al)-NH_2	35.92	19.80
MIL-53(Al)-NH_2	5.16	1.89
MIL-53(Al)	0.79	0.15
Blank (no catalyst)	8.1[b]	

[a] Calculated at conversion < 15%. [b] Blank yielded 8.1 wt.% glucose conversion after 2 h. Reaction condition: 5 wt.% glucose (0.05 g), 1 g ethanol, 120 °C.

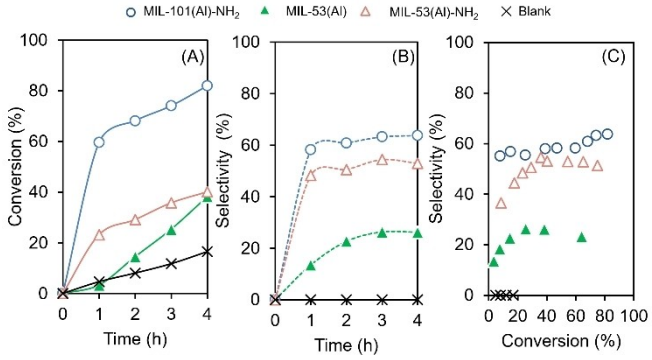

Figure 3. Glucose isomerization by selected Al-containing metal-organic frameworks. Glucose conversion (A), fructose selectivity (B) and relationship between fructose selectivity versus glucose conversion (C). Reaction condition: 5 wt.% glucose in ethanol (1 g), catalyst (glucose:metal molar ratio of 25:1), 120 °C.

indicated that amino-functionalized MOFs enhanced the catalytic activity and fructose selectivity. Given that the MIL-101(Al)-NH_2 exhibited the highest selectivity to fructose and glucose conversion, we examined MIL-101(Al)-NH_2 further.

Effects of Al-MOF precursors on glucose isomerization

To decouple the contribution of precursors of Al-MOF, we performed glucose isomerization with 2-aminoterephthalic acid (2-ATA, linker) and aluminum precursor ($AlCl_3$) in the form of a physical mixture at 120 °C for 2 h (Table 2). As a control, we conducted the same glucose isomerization experiment using 1,4-benzenedicarboxylic acid, the amino-free version of 2-aminoterephthalic acid. We found that 1,4-benzenedicarboxylic acid yielded 6% glucose conversion, which indicated that free –COOH groups were not active for glucose isomerization. Compared with 1,4-benzenedicarboxylic acid, 2-aminoterephthalic acid gave 79% glucose conversion. We observed a trace of fructose, 4.2% 5-hydroxymethylfurfural selectivity, and brown particles in the reaction mixture. These results suggested that the amino group made 2-aminoterephthalic acid more active and promoted side reactions, such as dehydration and degradation. The $AlCl_3$ catalyst showed 97% glucose conversion with 26% fructose selectivity. A physical mixture of $AlCl_3$ and 2-aminoterephthalic acid gave a moderate glucose conversion of 46% with slight fructose formation (3.5% fructose selectivity), whereas MIL-101(Al)-NH_2 exhibited 60.9% fructose selectivity at 68.2% glucose conversion. These results demonstrated the importance of coordinately unsaturated Al sites (CUS) in the amino-functional groups in MIL-101(Al)-NH_2 for good activity and selectivity in glucose isomerization.

Table 2. Catalytic activity of linker and ligands for the glucose isomerization in ethanol.

Entry	Catalyst	Conversion [mol%]	Product selectivity [mol%]	
			HMF	Fructose
1	$AlCl_3.6H_2O$[a]	96.6	1.1	26.0
2	2-ATA[a]	78.5	4.2	1.2
3	BDC[b]	6.0	0	0
4	$AlCl_3$ + 2-ATA[c]	46.0	2.5	3.5
5	MIL-101(Al)-NH_2	68.2	0	60.9

[a] $AlCl_3$ and 2-ATA were loaded with a similar Al and 2-ATA content to MIL-101(Al)-NH_2. [b] BDC (1,4-benzenedicarboxylic acid) was loaded based on similar terephthalic acid equivalent to 2-ATA. [c] $AlCl_3$ + 2-ATA were physically mixed with similar content to MIL-101(Al)-NH_2. Reaction condition: 5 wt.% glucose in ethanol (1 g), catalyst (glucose:metal molar ratio of 25:1), 120 °C, 2 h.

Effects of solvents on glucose isomerization by MIL-101(Al)-NH_2 catalyst

To determine the effect of solvents on catalytic performance, we performed glucose isomerization by MIL-101(Al)-NH_2 in (1) polar protic solvents (1-propanol, 2-propanol, 1-butanol, 2-butanol, methanol, ethanol, and water) and (2) polar aprotic solvents (dimethylacetamide (DMA), dimethyl sulfoxide (DMSO), and ethyl acetate) (Figure S2). The reaction in ethyl acetate gave the lowest fructose selectivity of 10.6% at 55.6% glucose conversion. The reaction by MIL-101(Al)-NH_2 in water gave a moderate fructose selectivity (35.4%) at 40.3% glucose conversion (see Supporting Information for detail, Table S3). Other polar aprotic solvents (DMA, DMF, and DMSO) and secondary alcohols (2-propanol and 2-butanol) gave inferior fructose selectivity and glucose conversion compared with those results from primary alcohols. Among primary alcohols, glucose isomerization in ethanol gave the highest fructose selectivity of 61% and glucose conversion of 68%. These results suggested that the coordination environment of solvents and acid sites of MIL-101(Al)-NH_2 affected its catalytic performance.

Stability and reusability of MIL-101(Al)-NH_2 in glucose isomerization

The ability to reuse catalysts is important for their practical use. We recovered the MIL-101(Al)-NH_2 by centrifugation and washing with water to remove the residual products, intermediates, and unreacted glucose. The catalyst was then dried in a vacuum oven at 130 °C to remove moisture. We selected this temperature based on our TGA results to minimize the decomposition of MIL-101(Al)-NH_2. The MIL-101(Al)-NH_2 catalyst maintained the catalytic performance with $<$9% drop in glucose conversion, and the catalyst retained its fructose selectivity (61%) for four cycles (Figure 4A). Further, after the 4th reuse cycle, we characterized the used MIL-101(Al)-NH_2 catalyst by ICP-OES, XRD, and FTIR (Figure S3). The aluminum content of the used catalyst, measured by ICP-OES, was 10.5 wt.%, essentially identical to that of the fresh catalysts (11.6 wt.%); thus, minimal aluminum leaching occurred even after 4 cycles. The XRD and FTIR spectra of the used catalyst exhibited chemical structure and functionality similar to fresh Al-MOF, which suggested minimal changes in chemical structure of the Al-MOF after reuse. Together, these recovery and character-

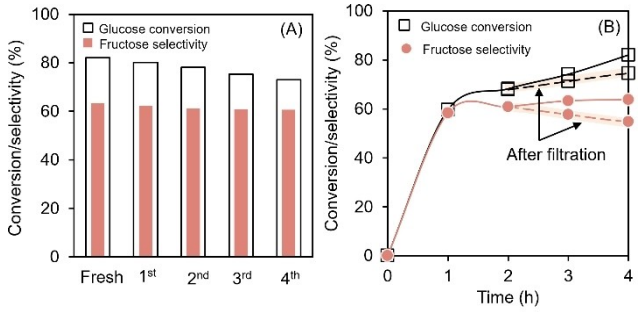

Figure 4. Reusability and stability of MIL-101(Al)-NH_2 for the glucose isomerization. Recycle test of MIL-101(Al)-NH_2 catalyst at 120 °C, 4 h (A), and filtration test after 1 h at 120 °C (B). A dashed line with orange highlight represents the reaction data after filtering the catalyst. An undashed line represents the reaction data without filtering the catalyst. Reaction condition: 5 wt.% glucose in ethanol (1 g), catalyst (glucose:metal molar ratio of 25:1), 120 °C.

ization results demonstrated catalyst stability under the present experimental conditions. Overall, MIL-101(Al)-NH_2 maintained high selectivity to fructose for all the cycles and structural integrity after four recycles.

To evaluate the catalyst stability under the reaction condition, we performed filtration experiments. Glucose isomerization was conducted for 1 h at 120 °C with MIL-101(Al)-NH_2, followed by filtering the MIL-101(Al)-NH_2 catalyst from the reaction mixture, and heating the filtrate under the same reaction condition (120 °C) for 4 h (Figure 4B). We sampled the reaction mixture three times during 4 h and monitored changes in glucose and fructose concentrations. The glucose conversion increased ~16%, in agreement with our blank experiment (no catalyst), which showed glucose conversion under the same experimental condition (Table 1). Whereas the fructose selectivity slightly decreased. These results suggested that little to no Al species leached from MIL-101(Al)-NH_2 into the reaction mixture.

Discussion

We discovered the amino-based aluminum-containing metal-organic frameworks (Al-MOFs) as active and selective catalysts for glucose isomerization to fructose. The current commercial glucose isomerization process uses the enzyme glucose isomerase. However, as with any enzymic process, the reaction conditions (pH and temperature) must be strictly controlled to maintain enzyme activity and stability; this requirement contributes to a high operating cost. We demonstrated that the MIL-101(Al)-NH_2 and MIL-53(Al)-NH_2 were selective for glucose isomerization and reached 64% fructose selectivity at 82% glucose conversion by MIL-101(Al)-NH_2 and 53% fructose selectivity at 75% glucose conversion by MIL-53(Al)-NH_2 at 120 °C in ethanol.

The most significant finding was that the incorporation of the amino group enhanced fructose selectivity of MIL-101(Al)-NH_2. The amino groups in the MOF structure enhanced medium-to-strong Lewis acid strength and promoted glucose conversion and fructose selectivity for glucose isomerization. The MIL-101(Al)-NH_2 catalyst showed catalytic activity similar to that of Sn-containing β-zeolite in glucose isomerization (Figure 5). In theory, the amino groups in the 2-aminoterephthalic acid linkers, electron-donating group, donate electron density to a conjugated π system by resonance or inductive effects, making the π system more nucleophilic. This increase in electron density of –COOH groups of 2-aminoterephthalic acid decreases the Lewis acid characters of coordinated unsaturated sites (CUSs) and catalytic activity of the reaction.[60–61] Because Lewis acid sites are the active sites for glucose isomerization, we should have observed lower activity and selectivity in –NH_2-containing MOFs.[60–62] However, lower activity was not the case for MIL-53(Al)-NH_2, which had a greater activity (glucose conversion) and fructose selectivity compared with its amino-free analog, MIL-53(Al).

Our results corroborated previous studies, which showed that amino groups of MOFs enhanced their catalytic activity for esterification,[22,63] condensation,[64–65] and photocatalysis reactions.[66] However, the origin of this enhancement by amino groups in MOFs has been debated. Caratelli et al.[63] and Hajek et al.[64] used quantum calculations to investigate the function of amino groups in UiO-66(Zr) and their contribution in esterification and aldol condensation reaction. They found that amino groups did not have a direct effect in the reaction mechanism. The location/orientation of the functional groups in the framework in different solvent environments affect the adsorption of reactants,[63] hydrophobicity/hydrophilicity of the catalytic sites, porosity, and accessibility to the metal sites.[62,67] These attributes contribute to the reactivity of MOFs in glucose isomerization. Future quantum calculation and molecular dynamic simulation studies will focus on decoupling the effect of Al sites and functional groups of Al-MOFs on glucose isomerization.

Coordination environments around metal centers and organic linkers significantly affect MOF stability and catalytic activity.[68–69] Guo et al.[70] used a $Cr(OH)_3$/MIL-101(Cr) composite catalyst and achieved 78% fructose selectivity at ~77% glucose

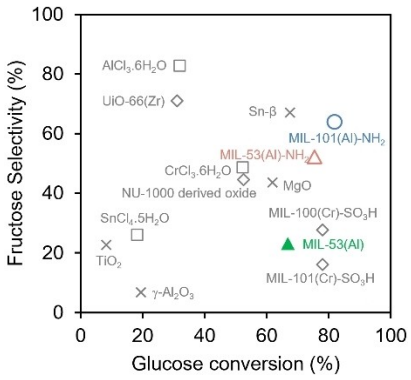

Figure 5. Selected catalysts for glucose isomerization reaction and their reactivity. These catalysts were used under different reaction conditions (glucose/catalyst loading, solvent, reaction temperature, and reaction time (see Supporting Information for detail, Table S1).[23,91–94]

conversion at 100 °C in ethanol. They achieved a high fructose selectivity and glucose conversion because of the combination of Lewis acidic MIL-101(Cr) and base-like chromium hydroxide sites. On the basis of our results and findings from previous studies, we postulated that the high fructose selectivity of MIL-101(Al)–NH_2 was due to the combination of hydride shift and proton transfer mechanisms. The Lewis acid sites of MIL-101 enabled the hydride shift mechanism to form fructose.[71] The –NH_2 group provided the Lewis base properties and hydrogen-bond donor ability,[72] which facilitated the proton transfer mechanism to produce fructose. In future studies with linker engineering and Density Functional Theory calculations, we will focus on elucidating the effect of a combination of Lewis acid and base sites on activity and selectivity of Al-MOFs on glucose isomerization.

Coordination environments of solvent molecules around catalysts' active sites affect the catalytic performance. Our reaction by MIL-101(Al)-NH_2 in primary alcohols yielded a high glucose conversion and fructose selectivity at 120 °C with the highest fructose selectivity of 61% and glucose conversion of 68% in ethanol. Researchers have investigated the effect of non-aqueous solvents on glucose-fructose isomerization because non-aqueous solvents can improve solubilities of reactants/products, conversion rates, and selectivities to desired products.[73–74] Such non-aqueous solvents include alcohols,[34,75] DMSO,[76] and DMA.[77–78] Yabushita et al.[79] reported superior fructose selectivity (>78%) and glucose conversion (>55%) by Mg–Al hydrotalcite in primary alcohols (methanol, ethanol, and 1-propanol) to those in water at 90 °C for 2 h. de Mello et al.[26] modulated UiO-66(Zr) to create Lewis acid sites for glucose isomerization in alcohols. They found that reaction in 1-propanol gave the highest fructose selectivity of 73% at 82% glucose conversion. The high catalytic activity of these catalysts in primary alcohols corroborated our results. Although the fructose selectivity by MIL-101(Al)-NH_2 in primary alcohols was slightly lower than modulated UiO-66(Zr) and Mg–Al hydrotalcite, we demonstrated that Al-MOF catalyst was stable and reusable at least four times.

Potential reasons for the high catalytic performance in primary alcohols of our MIL-101(Al)-NH_2 and other Lewis acidic catalysts were the following: (1) primary alcohols shifted the isomerization equilibrium to the fructose side, and (2) primary alcohols stabilized the transition-state species, which facilitated the glucose-fructose isomerization and suppressed undesired side reactions (humin formation).[34] Angyal et al.[80] found that ethanol changed the anomeric equilibrium of glucose, thereby changing the apparent chemical equilibrium and facilitating the isomerization of glucose. Visuri et al.[81] reported that adding ethanol to water shifted the isomerization equilibrium and increased the fructose concentration in its equilibrium mixture with glucose. Hu et al.[82] and Kochemann et al.[83] stabilized glucose/xylose-derived reactive intermediates by adding short-chain alcohols (methanol and ethanol), which suppressed the undesired humin formation. These previous results agree with our finding of the highest catalytic performance of MIL-101(Al)-NH_2 in primary alcohols.

Our findings demonstrated that MIL-101(Al)-NH_2 was an active, selective, and stable catalyst for glucose isomerization in ethanol. In Figure 5, we summarize the activity of selected catalysts for glucose isomerization to fructose. The MIL-101(Al)-NH_2 catalyst was superior to other MOFs because of high catalytic activity and fructose selectivity.

The synthesis procedures of Al-MOFs are simple with catalytic performance for glucose isomerization comparable to the solid catalyst alternative, Sn-containing zeolites.[8–12] Our findings offer a new understanding of how amino groups increase Lewis acid strength, and the findings could guide the development of reusable selective catalysts for glucose isomerization. Moreover, this new understanding is expected to extend to other Lewis acid-catalyzed organic reactions,[84] such as Diels-Alder,[85] Meerwein-Ponndorf-Verley,[86–87] oxidation,[62] Friedel-Crafts,[88–89] hydration,[90] and production of 5-hydroxymethylfurfural from cellulose.[10]

Conclusion

We demonstrated the viability of aluminum-containing metal organic frameworks (Al-MOFs) for glucose isomerization to fructose in ethanol, and eliminated concerns about selectivity, stability, and reuse of the catalysts. MIL-101(Al)–NH_2 yielded 64% fructose selectivity at 82% glucose conversion at 120 °C. The MIL-101(Al)-NH_2 retained its catalytic performance after reusing four times. These results provide a new perspective in the application of Al-MOFs for production of fructose from renewable glucose for biorefineries. Moreover, the knowledge gained about the solvent effect will help in designing active and selective MOF catalytic systems for glucose-fructose isomerization.

Experimental Section

Materials

Table S4 lists the manufacturers, CAS numbers, and purities of chemicals, reagents, and solvents used in this study. All chemicals, solvents, and gases were used as received, unless otherwise noted.

Synthesis of metal-organic frameworks

MIL-101(Al)-NH_2 and MIL-53(Al)-H/NH_2 were synthesized by solvothermal methods (see Supporting Information for detail).

Characterization of the metal-organic framework

The synthesized MOFs were characterized by X-ray diffraction (XRD), nitrogen adsorption-desorption, attenuated total reflectance-Fourier-transform infrared spectroscopy (ATR-FTIR), thermogravimetric analysis (TGA), high-resolution transmission electron microscopy (HRTEM), and inductively coupled plasma-optical emission spectroscopy (ICP-OES) (see Supporting Information for detail).

Determination of acid sites by diffuse reflectance infrared Fourier transform spectroscopy

Diffuse reflectance infrared Fourier transform spectroscopy (DRIFTS) with adsorbed pyridine was performed to characterize the acid sites. The temperature-programmed desorption was conducted with the JASCO FTIR equipped with a high-temperature DiffuseIR™ cell (PIKE Technology, WI, USA). The sample treatment and DRIFTS experiments with temperature-programmed desorption were conducted with a slight modification as described.[95] In short, the MOF sample (~5 mg) was placed in a cylindrical alumina crucible and treated in N_2 gas (50 mL/min) at 130 °C for 60 min unless otherwise noted. After the pretreatment, the sample was cooled to 30 °C. The DRIFT spectrum of fresh catalyst was recorded as the background spectrum. The samples were then saturated with pyridine vapor by the flow of N_2 gas (50 mL/min). Then the physisorbed pyridine was removed by flushing with N_2 gas (50 mL/min) at 50, 100, or 150 °C for 30 min before recording the DRIFT spectra. Because of the limited thermal stability of Al-MOF, a lower desorption temperature (maximum 150 °C) was used. All spectra were recorded with 256 scans between 4000–400 cm^{-1} at a 4 cm^{-1} resolution. The amount of Lewis acid sites at each desorption temperature was calculated from the integrated area of bands (after background subtraction) of adsorbed pyridine at 1067 cm^{-1}. This Lewis acid determination was adapted from Yu et al.[57] A cascade increase in the desorption temperature from 30–150 °C enables identification of weak and medium to strong Lewis acid sites of MOFs. The Lewis acid peaks at 150 °C implied the medium-to-strong Lewis acid sites because of a strong coordination between pyridine and Lewis acid sites at a high desorption temperature. The Lewis acid peaks at 30 °C indicated the combination of weak and medium-to-strong Lewis acid sites. To calculate the weak Lewis acid sites, Lewis acid peak area at 150 °C was subtracted from that at 30 °C.

Isomerization of glucose

To evaluate the catalysts, the glucose isomerization reaction was conducted with 25 mL pressure tubes in an oil bath. Briefly, 5 wt.% glucose in solvent (1 mL) and catalyst (glucose:metal molar ratio of 25:1) were added to pressure tubes, which were sealed and stirred at 120 °C. Xylitol was added as an external standard to the solution of reactants and products after completing the reaction. The reaction was stopped by quenching in a cold-water bath followed by adding water (5 mL) to dissolve the remaining glucose and solvents. The solution was centrifuged, and the solid catalyst was removed. The liquid sample was then analyzed using High-Pressure Liquid Chromatography (HPLC).

Product analysis and quantification

The reactants and products were analyzed with an HPLC (Agilent Technology, Santa Clara, CA, USA) equipped with a refractive index detector (RID) and diode array detector (DAD). An Aminex HPX-87H column (300×7.8 mm, Bio-Rad®, Hercules, CA, USA) was used for reactant and product separation at 60 °C with 0.6 mL/min of 4 mM H_2SO_4 as the mobile phase. Selected samples were separated and analyzed for mannose by Aminex HPX-87P column (300×7.8 mm, Bio-Rad®, Hercules, CA, USA) and RID as previously described[96] (see Supporting Information and Figure S4 for detail). The concentrations of sugars were determined by the peak area from the RID signals. The concentrations of hydroxymethylfurfural were determined by the peak area from the DAD signals at 280 nm wavelength as described.[97] All reactants and products were calibrated against certified standards (Absolute Standards, Inc., Hamden, CT, USA). Mannose was not detected in all reaction mixtures. The glucose conversion, product yield, and product selectivity were calculated as follows:

$$\text{Glucose conversion } (\%) = \frac{\text{glucose reacted (mol)}}{\text{initial glucose (mol)}} \times 100$$

$$\text{Product yield } (\%) = \frac{\text{product formed (mol)}}{\text{initial glucose (mol)}} \times 100$$

$$\text{Product selectivity } (\%) = \frac{\text{product yield } (\%)}{\text{glucose conversion } (\%)} \times 100$$

Specific activity and productivity were used to express the rate per metal site at which glucose was consumed, and fructose was formed, respectively. They were calculated at low glucose conversion (< 15%) to ensure that there were no side reactions;[98] the following expressions were used.

$$\text{Specific activity } (h^{-1}) = \frac{\text{glucose reacted (mol)}}{\text{metal (mol)} \times \text{time (h)}}$$

$$\text{Productivity } (h^{-1}) = \frac{\text{fructose formed (mol)}}{\text{metal (mol)} \times \text{time (h)}}$$

Catalyst reusability

For the MOF recycling tests, the spent catalysts were collected by centrifugation of the reaction mixture, and the liquid portion was decanted for HPLC analysis. The solid catalyst was washed twice with 5 mL of ethanol and twice with 5 mL of water to remove residual reactants and products. The solid catalyst was then separated by centrifugation and dried in a vacuum oven at 120 °C overnight before reuse.

Acknowledgements

A part of this material is based upon work supported by the National Science Foundation under Cooperative Agreement No. 1355438 and Internal Research Grant, Office of the Executive Vice President for Research, University of Louisville. This work was performed in part at the Conn Center for Renewable Energy Research at the University of Louisville, which belongs to the National Science Foundation NNCI KY Manufacturing and Nano Integration Node, supported by ECCS-1542174. The authors would like to thank Dr. Howard Fried for his valuable comments and suggestions on the manuscript.

Conflict of Interest

The authors declare no conflict of interest.

Data Availability Statement

The data that support the findings of this study are available from the corresponding author upon reasonable request.

Keywords: amino group · fructose · glucose isomerization · Lewis acids · metal-organic frameworks

[1] Y. Park, E. Yetley, *Am. J. Clin. Nutr.* **1993**, *58*, 737S-747S.
[2] B. Kamm, *Angew. Chem. Int. Ed.* **2007**, *46*, 5056–5058; *Angew. Chem.* **2007**, *119*, 5146–5149.
[3] N. Rodriguez Quiroz, A. Norton, H. Nguyen, E. Vasileiadou, D. Vlachos, *ACS Catal.* **2019**, *9*, 9923–9952.
[4] J. Lecomte, A. Finiels, C. Moreau, *Starch/Staerke* **2002**, *54*, 75–79.
[5] V. Jensen, S. Rugh, *Methods Enzymol.* **1987**, *136*, 356–370.
[6] Y. Tewari, *Appl. Biochem. Biotechnol.* **1990**, *23*, 187–203.
[7] R. Messing, A. Filbert, *J. Agric. Food Chem.* **1975**, *23*, 920–923.
[8] M. Moliner, Y. Román-Leshkov, M. E. Davis, *PNAS* **2010**, *107*, 6164–6168.
[9] Y. Román-Leshkov, M. Moliner, J. A. Labinger, M. E. Davis, *Angew. Chem. Int. Ed.* **2010**, *49*, 8954–8957; *Angew. Chem.* **2010**, *122*, 9138–9141.
[10] Q. Guo, L. Ren, S. Alhassan, M. Tsapatsis, *Chem. Commun.* **2019**, *55*, 14942–14945.
[11] L. Ren, Q. Guo, P. Kumar, M. Orazov, D. Xu, S. Alhassan, K. Mkhoyan, M. Davis, M. Tsapatsis, *Angew. Chem. Int. Ed.* **2015**, *127*, 10998–11001.
[12] J. Pimenta Lorenti, E. Scolari, N. Cabral, C. Bisio, J. Gallo, *Ind. Eng. Chem. Res.* **2021**, *60*, 12821–12833.
[13] W. van der Graaff, C. Tempelman, E. Pidko, E. Hensen, *Catal. Sci. Technol.* **2017**, *7*, 3151–3162.
[14] H. Furukawa, K. E. Cordova, M. O'Keeffe, O. M. Yaghi, *Science* **2013**, *341*, 1230444.
[15] J. Lee, O. K. Farha, J. Roberts, K. A. Scheidt, S. T. Nguyen, J. T. Hupp, *Chem. Soc. Rev.* **2009**, *38*, 1450–1459.
[16] D. Farrusseng, S. Aguado, C. Pinel, *Angew. Chem. Int. Ed.* **2009**, *48*, 7502–7513; *Angew. Chem.* **2009**, *121*, 7638–7649.
[17] J. Hall, P. Bollini, *ACS Catal.* **2020**, *10*, 3750–3763.
[18] F. Zhang, J. Shi, Y. Jin, Y. Fu, Y. Zhong, W. Zhu, *Chem. Eng. J.* **2015**, *259*, 183–190.
[19] A. Valekar, M. Lee, J. Yoon, J. Kwak, D.-Y. Hong, K.-R. Oh, G.-Y. Cha, Y.-U. Kwon, J. Jung, J.-S. Chang, *ACS Catal.* **2020**, *10*, 3720–3732.
[20] S. Rojas-Buzo, P. García-García, A. Corma, *ChemSusChem* **2018**, *11*, 432–438.
[21] Y. Sun, L. Shi, H. Wang, G. Miao, L. Kong, S. Li, Y. Sun, *Sustain. Energy Fuels* **2019**, *3*, 1163–1171.
[22] F. Cirujano, A. Corma, F. Xamena, *Catal. Today* **2015**, *257*, 213–220.
[23] R. Oozeerally, D. L. Burnett, T. W. Chamberlain, R. I. Walton, V. Degirmenci, *ChemCatChem* **2018**, *10*, 706–709.
[24] M. D. de Mello, M. Tsapatsis, *ChemCatChem* **2018**, *10*, 2417–2423.
[25] G. Akiyama, R. Matsuda, H. Sato, S. Kitagawa, *Chemistry–An Asian Journal* **2014**, *9*, 2772–2777.
[26] M. D. de Mello, *ChemCatChem* **2018**, *10*, 2417–2423.
[27] R. Oozeerally, *ChemCatChem* **2018**, *10*, 706–709.
[28] G. Akiyama, *Chemistry–An Asian Journal* **2014**, *9*, 2772–2777.
[29] M. Yabushita, P. Li, T. Islamoglu, H. Kobayashi, A. Fukuoka, O. K. Farha, A. Katz, *Ind. Eng. Chem. Res.* **2017**, *56*, 7141–7148.
[30] R. Oozeerally, S. D. K. Ramkhelawan, D. L. Burnett, C. H. L. Tempelman, V. Degirmenci, *Catalysts* **2019**, *9*, 812.
[31] V. Choudhary, A. Pinar, R. Lobo, D. Vlachos, S. Sandler, *ChemSusChem* **2013**, *6*, 2369–2376.
[32] A. Norton, H. Nguyen, N. Xiao, D. Vlachos, *RSC Adv.* **2018**, *8*, 17101–17109.
[33] C. Rasrendra, I. Makertihartha, S. Adisasmito, H. Heeres, *Top. Catal.* **2010**, *53*, 1241–1247.
[34] M. Yabushita, N. Shibayama, K. Nakajima, A. Fukuoka, *ACS Catal.* **2019**, *9*, 2101–2109.
[35] T. Vuorinen, E. Sjöström, *Carbohydr. Res.* **1982**, *108*, 23–29.
[36] K. Visuri, A. Klibanov, *Biotechnol. Bioeng.* **1987**, *30*, 917–920.
[37] T. Zhao, I. Boldog, V. Spasojevic, A. Rotaru, Y. Garcia, C. Janiak, *J. Mater. Chem. C* **2016**, *4*, 6588–6601.
[38] M. Sánchez-Sánchez, N. Getachew, K. Díaz, M. Díaz-García, Y. Chebude, I. Díaz, *Green Chem.* **2015**, *17*, 1500–1509.
[39] Y. Luan, Y. Qi, H. Gao, R. S. Andriamitantsoa, N. Zheng, G. Wang, *J. Mater. Chem. A* **2015**, *3*, 17320–17331.
[40] D. V. Patil, P. B. S. Rallapalli, G. P. Dangi, R. J. Tayade, R. S. Somani, H. C. Bajaj, *Ind. Eng. Chem. Res.* **2011**, *50*, 10516–10524.
[41] C. Li, Z. Xiong, J. Zhang, C. Wu, *J. Chem. Eng. Data* **2015**, *60*, 3414–3422.
[42] R. Huang, X. Guo, S. Ma, J. Xie, J. Xu, J. Ma, *Polymer* **2020**, *12*, 108.
[43] L. Bromberg, X. Su, T. A. Hatton, *ACS Appl. Mater. Interfaces* **2013**, *5*, 5468–5477.
[44] T. Toyao, M. Fujiwaki, Y. Horiuchi, M. Matsuoka, *RSC Adv.* **2013**, *3*, 21582–21587.
[45] E. V. Ramos-Fernandez, C. Pieters, B. van der Linden, J. Juan-Alcañiz, P. Serra-Crespo, M. Verhoeven, H. Niemantsverdriet, J. Gascon, F. Kapteijn, *J. Catal.* **2012**, *289*, 42–52.
[46] P. Serra-Crespo, E. V. Ramos-Fernandez, J. Gascon, F. Kapteijn, *Chem. Mater.* **2011**, *23*, 2565–2572.
[47] V. I. Isaeva, A. L. Tarasov, L. E. Starannikova, Y. P. Yampol'skii, A. Y. Alent'ev, L. M. Kustov, *Russ. Chem. Bull.* **2015**, *64*, 2791–2795.
[48] B. Seoane, C. Téllez, J. Coronas, C. Staudt, *Sep. Purif. Technol.* **2013**, *111*, 72–81.
[49] X.-X. Zheng, Z.-P. Fang, Z.-J. Dai, J.-M. Cai, L.-J. Shen, Y.-F. Zhang, C.-T. Au, L.-L. Jiang, *Inorg. Chem.* **2020**, *59*, 4483–4492.
[50] C. Volkringer, H. Leclerc, J.-C. Lavalley, T. Loiseau, G. Ferey, M. Daturi, A. Vimont, *J. Phys. Chem. C* **2012**, *116*, 5710–5719.
[51] H. Leclerc, A. Vimont, J.-C. Lavalley, M. Daturi, A. Wiersum, P. Llwellyn, P. Horcajada, G. Férey, C. Serre, *Phys. Chem. Chem. Phys.* **2011**, *13*, 11748–11756.
[52] Y. P. Xu, Z. Q. Wang, H. Z. Tan, K. Q. Jing, Z. N. Xu, G. C. Guo, *Catal. Sci. Technol.* **2020**, *10*, 1699–1707.
[53] M. A. Hossain, K. N. Mills, A. M. Molley, M. S. Rahaman, S. Tulaphol, S. B. Lalvani, J. Dong, M. K. Sunkara, N. Sathitsuksanoh, *Appl. Catal. A* **2021**, *611*, 117979.
[54] S. Roy, K. Bakhmutsky, E. Mahmoud, R. F. Lobo, R. J. Gorte, *ACS Catal.* **2013**, *3*, 573–580.
[55] T. Montanari, E. Finocchio, G. Busca, *J. Phys. Chem. C* **2011**, *115*, 937–943.
[56] T. K. Phung, M. M. Carnasciali, E. Finocchio, G. Busca, *Appl. Catal. A* **2014**, *470*, 72–80.
[57] D. Yu, M. Wu, Q. Hu, L. Wang, C. Lv, L. Zhang, *J. Hazard. Mater.* **2019**, *367*, 456–464.
[58] K. Góra-Marek, K. Tarach, M. Choi, *J. Phys. Chem. C* **2014**, *118*, 12266–12274.
[59] B. Chakraborty, B. Viswanathan, *Catal. Today* **1999**, *49*, 253–260.
[60] M. Timofeeva, V. Panchenko, J. Jun, Z. Hasan, M. Matrosova, S. Jhung, *Appl. Catal. A* **2014**, *471*, 91–97.
[61] F. Vermoortele, M. Vandichel, B. Van de Voorde, R. Ameloot, M. Waroquier, V. Van Speybroeck, D. De Vos, *Angew. Chem. Int. Ed.* **2012**, *51*, 4887–4890; *Angew. Chem.* **2012**, *124*, 4971–4974.
[62] J. Moreno, A. Velty, U. Díaz, A. Corma, *Chem. Sci.* **2019**, *10*, 2053–2066.
[63] C. Caratelli, J. Hajek, F. Cirujano, M. Waroquier, F. Xamena, V. Speybroeck, *J. Catal.* **2017**, *352*, 401–414.
[64] J. Hajek, M. Vandichel, B. Van de Voorde, B. Bueken, D. De Vos, M. Waroquier, V. Van Speybroeck, *J. Catal.* **2015**, *331*, 1–12.
[65] V. Panchenko, M. Matrosova, J. Jeon, J. Jun, M. Timofeeva, S. Jhung, *J. Catal.* **2014**, *316*, 251–259.
[66] L. Shen, R. Liang, M. Luo, F. Jing, L. Wu, *Phys. Chem. Chem. Phys.* **2015**, *17*, 117–121.
[67] T. Devic, P. Horcajada, C. Serre, F. Salles, G. Maurin, B. Moulin, D. Heurtaux, G. Clet, A. Vimont, J.-M. Greneche, *JACS* **2010**, *132*, 1127–1136.
[68] A. Goswami, D. Ghosh, V. Chernyshev, A. Dey, D. Pradhan, K. Biradha, *ACS Appl. Mater. Interfaces* **2020**, *12*, 33679–33689.
[69] Z. Huang, F. Zhao, L. Fan, W. Zhao, B. Chen, X. Chen, S.-F. Zhou, J. Xiao, G. Zhan, *Mater. Des.* **2020**, *194*, 108881.
[70] Q. Guo, L. Ren, P. Kumar, V. J. Cybulskis, K. A. Mkhoyan, M. E. Davis, M. Tsapatsis, *Angew. Chem. Int. Ed.* **2018**, *130*, 5020–5024.
[71] Q. X. Luo, Y. B. Zhang, L. Qi, S. Scott, *ChemCatChem* **2019**, *11*, 1903–1909.
[72] Z. Gao, X. Zhang, P. Xu, J. Sun, *Inorg. Chem. Front.* **2020**, *7*, 1995–2005.
[73] L. Shuai, J. Luterbacher, *ChemSusChem* **2016**, *9*, 133–155.
[74] M. Mellmer, C. Sanpitakseree, B. Demir, P. Bai, K. Ma, M. Neurock, J. Dumesic, *Nat. Catal.* **2018**, *1*, 199–207.
[75] M. de Mello, M. Tsapatsis, *ChemCatChem* **2018**, *10*, 2417–2423.
[76] R.-J. van Putten, J. Van Der Waal, E. De Jong, C. Rasrendra, H. Heeres, J. de Vries, *Chem. Rev.* **2013**, *113*, 1499–1597.
[77] A. Marianou, C. Michailof, A. Pineda, E. Iliopoulou, K. Triantafyllidis, A. Lappas, *ChemCatChem* **2016**, *8*, 1100–1110.
[78] S. An, D. Kwon, J. Cho, J. Jung, *Catalysts* **2020**, *10*, 1236.
[79] M. Yabushita, *ACS Catal.* **2019**, *9*, 2101–2109.
[80] S. J. Angyal, *Angew. Chem. Int. Ed.* **1969**, *8*, 157–166; *Angew. Chem.* **1969**, *81*, 172–182.
[81] K. Visuri, *Biotechnol. Bioeng.* **1987**, *30*, 917–920.
[82] X. Hu, C.-Z. Li, *Green Chem.* **2011**, *13*, 1676–1679.

[83] J. Köchermann, J. Schreiber, M. Klemm, *ACS Sustainable Chem. Eng.* **2019**, *7*, 12323–12330.
[84] A. Corma, H. García, *Chem. Rev.* **2003**, *103*, 4307–4366.
[85] P. Vermeeren, M. D. Tiezza, M. van Dongen, I. Fernández, F. Bickelhaupt, T. Hamlin, *ChemCatChem* **2021**, *27*, 10610–10620.
[86] Y. Lin, Q. Bu, J. Xu, X. Liu, X. Zhang, G.-P. Lu, B. Zhou, *J. Mol. Catal.* **2021**, *502*, 111405.
[87] A. Corma, M. Domine, L. Nemeth, S. Valencia, *J. Am. Chem. Soc.* **2002**, *124*, 3194–3195.
[88] P. Tarakeshwar, J. Lee, K. Kim, *J. Phys. Chem. A* **1998**, *102*, 2253–2255.
[89] E. Hall, L. Redfern, M. Wang, K. Scheidt, *ACS Catal.* **2016**, *6*, 3248–3252.
[90] M. Rahaman, S. Tulaphol, K. Mills, A. Molley, M. Hossain, S. Lalvani, T. Maihom, M. Crocker, N. Sathitsuksanoh, *ChemCatChem* **2022**, DOI: 10.1002/cctc.202101756.
[91] J. Tang, X. Guo, L. Zhu, C. Hu, *ACS Catal.* **2015**, *5*, 5097–5103.
[92] A. A. Marianou, C. M. Michailof, A. Pineda, E. F. Iliopoulou, K. S. Triantafyllidis, A. A. Lappas, *ChemCatChem* **2016**, *8*, 1100–1110.
[93] G. Akiyama, R. Matsuda, H. Sato, S. Kitagawa, *Chem. Asian J.* **2014**, *9*, 2772–2777.
[94] C. D. Malonzo, S. M. Shaker, L. Ren, S. D. Prinslow, A. E. Platero-Prats, L. C. Gallington, J. Borycz, A. B. Thompson, T. C. Wang, O. K. Farha, J. T. Hupp, C. C. Lu, K. W. Chapman, J. C. Myers, R. L. Penn, L. Gagliardi, M. Tsapatsis, A. Stein, *J. Am. Chem. Soc.* **2016**, *138*, 2739–2748.
[95] A. I. Osman, J. K. Abu-Dahrieh, D. W. Rooney, S. A. Halawy, M. A. Mohamed, A. Abdelkader, *Appl. Catal. B* **2012**, *127*, 307–315.
[96] M. Hossain, M. Rahaman, D. Lee, T. Phung, C. Canlas, B. Simmons, S. Renneckar, W. Reynolds, A. George, S. Tulaphol, N. Sathitsuksanoh, *Ind. Eng. Chem. Res.* **2019**.
[97] M. Rahaman, S. Tulaphol, M. Hossain, J. Jasinski, N. Sun, A. George, B. Simmons, T. Maihom, M. Crocker, N. Sathitsuksanoh, *Fuel* **2022**, *310*, 122459.
[98] S. Kozuch, J. Martin, *ACS Catal.* **2012**.

Manuscript received: January 27, 2022
Revised manuscript received: May 24, 2022
Accepted manuscript online: May 27, 2022
Version of record online: ■■, ■■■

RESEARCH ARTICLE

Selective glucose isomerization to fructose by aluminum-containing metal-organic frameworks: Al-MOFs are active catalysts for glucose isomerization to fructose in ethanol. Amino groups in Al-MOF enhance the Lewis acid site's strength and fructose selectivity. MIL-101(Al)-NH_2 is stable and reusable.

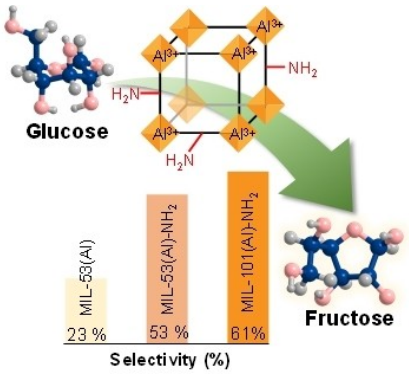

*M. S. Rahaman, Dr. S. Tulaphol, A. Hossain, Dr. J. B. Jasinski, Prof. S. B. Lalvani, Prof. M. Crocker, Dr. T. Maihom, Prof. N. Sathitsuksanoh**